Using Dysprosium Complexes To Probe the Nitrogenase Paramagnetic Centers†

Melinda E. Oliver and Brian J. Hales*

Department of Chemistry, Louisiana State University, Baton Rouge, Louisiana 70803-1804

Received November 19, 1992

ABSTRACT: EPR progressive power saturation techniques were used to monitor relaxation enhancement of the nitrogenase paramagnetic centers produced by interaction with Dy^{3+} complexes. Three models are presented for the relationship between the degree of enhancement and the distance of closest approach of Dy^{3+} to the intrinsic metal cluster. In the first model, the perturbing dysprosium ions are represented as a single average site. The second and third models are variations of the treatment of Innes and Brudvig [(1989) *Biochemistry 28*, 1116–1125] and assume the unknown protein to be spherical with Dy^{3+} dispersed either randomly over the surface of the protein or randomly in solution. Using these models, the distance of closest approach of the Dy^{3+} complex to the [4Fe-4S] cluster in the Fe-protein from *Azotobacter vinelandii* was determined to be 5.0–6.5 Å. Similary, the distance of closest approach to FeMoco in the MoFe-protein was determined to be 0.0–1.2 Å, which, when corrected to the fact that FeMoco exists as an $S = {}^3/_2$ spin state, indicates that the distance is ≥6 Å. These distances did not change when (1) either protein was in the presence of the other, (2) both proteins were cross-linked to each other, or (3) the Fe-protein from *A. vinelandii* was mixed with the MoFe-protein from *Clostridium pasteurianum*. On the other hand, formation of the inactive complex of the Fe-protein from *C. pasteurianum* with the MoFe-protein from *A. vinelandii* blocked dysprosium-induced relaxation enhancement, implying that each component protein overlaps the metal cluster in the complementing protein.

Nitrogenase consists of two separable proteins called component 1 and component 2. In the conventional form of the enzyme, component 1 (or MoFe-protein) contains both Mo and Fe in two different metal clusters, termed P-clusters and M-centers (Zimmermann et al., 1978). The structure of these clusters recently has been proposed (Kim & Rees, 1992b) where the P-clusters consist of a pair of bridged [4Fe-4S] clusters and the M-centers are oblate spheroids with Mo at one end and a suggested composition $MoFe_7S_8$. In the as-isolated form of the enzyme, the M-centers (also called the FeMo-cofactor or FeMoco)[1] are paramagnetic with an $S = {}^3/_2$ spin state while the P-clusters are diamagnetic (Münck et al., 1975). Upon oxidation with thionine, the M-centers become diamagnetic (Zimmermann et al., 1978) while the P-clusters convert to a paramagnetic, but EPR-silent, state with a probable spin of $S = {}^5/_2$–${}^7/_2$ (Johnson et al., 1981). Component 2 is a simpler protein, consisting of a pair of identical subunits which are bridged by a single [4Fe-4S] cluster (Georgiadis et al., 1990, 1992).

During enzymatic activity, component 2 (or Fe-protein) is reduced, binds MgATP, and associates with component 1, where it transfers one electron, hydrolyzes the MgATP, and dissociates from component 1 to start a new cycle. X-ray diffraction studies are currently in progress on the crystal structures of both proteins (Bolin et al., 1990; Georgiadis et al., 1990, 1992; Kim & Rees, 1992a,b). However, little is known concerning the degree of interaction between the clusters of the nitrogenase proteins during catalysis or the proximity of these clusters to the solvent environment when the individual proteins are in solution. In a previous paper (Oliver & Hales, 1992), EPR spectroscopy was used to probe the magnetic interactions between the P-clusters and M-centers during partial oxidation of component 1 and found that the P-clusters exist as interactive pairs that oxidize in one-electron steps.

In the present study, Dy^{3+} complexes are used to probe the M-center of component 1 (Av1) and the [4Fe-4S] cluster of component 2 (Av2) nitrogenase from *Azotobacter vinelandii*. The paramagnetism of this lanthanide enhances the spin–lattice relaxation rate of the intrinsic metal cluster, as monitored by the progressive power saturation technique. The relationship between the degree of this enhancement and the distance of closest approach of the lanthanide to the cluster will be described in terms of three different models.

MATERIALS AND METHODS

Materials and Preparations. Both component proteins of nitrogenase from *A. vinelandii* were isolated and purified using a variation (Hales et al., 1986) of published procedures (Burgess et al., 1980). Nitrogenase isolated from *Clostridium pasteurianum* (Cp1 and Cp2) was generously donated by Dr. Richard Barr (Exxon Research Laboratories, Annandale, NJ). Using acetylene reduction as a monitor of activity, specific activities (in units of nanomoles of C_2H_2 reduced per minute per milligram of protein) for the different proteins used in this study were 1800 (Av1), 1500 (Av2), 2200 (Cp1), and 1700 (Cp2).

Water-soluble 1-ethyl-3-[3-(dimethylamino)propyl]carbodiimide (EDC, Sigma) was used to cross-link Av1 and Av2 according to published procedures (Willing et al., 1989). Specifically, Av1 and Av2 in a 1:2 mole ratio were placed in identical EPR tubes containing a fresh solution of 12 mM EDC. In one of the tubes, DyEDTA (Dy obtained as $DyCl_3$, Sigma) was also added to a final concentration of 1.0 mM. In all of these samples, SDS–PAGE of the cross-linked proteins revealed the presence of a band at $M_r = 97\,000$, demonstrating the existence (Willing et al., 1989) of cross-linking between the two component proteins.

† This work was supported by the National Institutes of Health (Grant GM 33965).

[1] Abbreviations: Av1, nitrogenase MoFe-protein from *Azotobacter vinelandii*; Av2, nitrogenase Fe-protein from *A. vinelandii*; Cp1, MoFe-protein from *Clostridium pasteurianum*; Cp2, Fe-protein from *Clostridium pasteurianum*; EDC, 1-ethyl-3-[3-(dimethylamino)propyl]carbodiimide; FeMoco, Fe- and Mo-containing cofactor (also known as the M-center) from the nitrogenase MoFe-protein.

0006-2960/93/0432-6058$04.00/0

Cytochrome *c* was obtained from Sigma and used without further purification.

EPR Spectroscopy. EPR spectra were recorded on a Bruker ER300D spectrometer interfaced to a Bruker 1600 computer for data storage and manipulation. Low temperatures were achieved using an Oxford Instrument ESR-9 flow cryostat (3.8–300 K) positioned in a TE_{102} cavity, resonating at X-band frequencies. Temperatures were monitored using an Oxford Instruments Model ITC4 temperature controller with a digital readout.

For power saturation studies, all protein samples contained 0.1 M NaCl. To each of these samples was added 0.2–10 mM DyEDTA or LaEDTA (obtained as $LaCl_3$, Sigma) as a diamagnetic control. During each series of experiments, the temperature of the Oxford cryostat was maintained to ±0.1 K, and the microwave power settings were randomly chosen to avoid possible systematic error.

Magnetic Dipolar Interactions: Theory. In biological samples, a major source of interaction between two paramagnetic species (*i* and *j*) arises from dipolar coupling. The interaction energy ($\mathcal{H}_{ij}$) between a pair of dipoles (μ_i and μ_j) separated by a distance vector **r** can be written as

$$\mathcal{H}_{ij} = [(\mu_i \cdot \mu_j) - e(\mu_i \cdot \mathbf{r})(\mu_j \cdot \mathbf{r})/r^2]/r^3 \quad (1)$$

In the presence of a large external magnetic field (B_0), μ_i and μ_j precess with angular frequencies ω_i and ω_j and spin–lattice relaxation times T_{1i} and T_{1j}, respectively. In this situation, the resultant magnetic field experienced by species *i* is the sum of the static field B_0 plus a time-dependent local field produced by the relaxation, or spin-flipping, of *j* at a rate $1/T_{1j}$. Because species *j* is coupled to species *i*, it will induce relaxation in it.

Bloembergen (1949) and Abragam (1955) derived the expression showing the influence that paramagnetic species *j* has on the spin–lattice relaxation rate of species *i* when the two are coupled by magnetic dipolar interactions:

$$(1/T_{1i})_{\text{dipolar}} = J_j(J_j + 1)\{{}^1/_3 b^2_{ij}[2T_{1j}/(1 + (\omega_i - \omega_j)^2 T^2_{1j})] + {}^2/_3 c^2_{ij}[2T_{1j}/(1 + \omega^2_i T^2_{1j})] + {}^2/_3 e^2_{ij}[2T_{1j}/(1 + (\omega_i + \omega_j)^2 T^2_{1j})]\} \quad (2)$$

where

$$b^2_{ij} = {}^1/_4 \gamma_i^2 \gamma_j^2 h^2 r^{-6}(1 - 3\cos^2\phi_{ij})^2$$

$$c^2_{ij} = {}^9/_4 \gamma_i^2 \gamma_j^2 h^2 r^{-6} \sin^2\phi_{ij} \cos^2\phi_{ij}$$

$$e^2_{ij} = {}^9/_8 \gamma_i^2 \gamma_j^2 h^2 r^{-6} \sin^4\phi_{ij}$$

and ϕ_{ij} is the angle subtended by **r** and the direction of the external magnetic field while J_j is the total angular momentum of species *j* and γ_j its magnetogyric ratio.

Progressive Power Saturation. Portis (1953) and Castner (1959) first evaluated the relationship between power saturation and relaxation times of paramagnetic resonances. In general, the amplitude, *A*, of the derivative EPR spectrum is related to the incident microwave power, *P*, by the expression

$$A = K\sqrt{P}/(1 + P/P_{1/2})^{b/2} \quad (3)$$

where

$$P_{1/2} = 1/g^2 T_1 T_2$$

and *K* is a proportionality factor, $P_{1/2}$ is the microwave power needed for half-saturation of the signal, and T_2 is the spin–spin relaxation time. Exponent *b* in eq 3 is referred to as the inhomogeneity factor. For inhomogeneously broadened (Gaussian) lines, such as those observed for most metalloproteins, $b = 1$, while homogeneously broadened (Lorentzian) lines yield $b = 3$.

Equation 3 can be rearranged (Beinert & Orme-Johnson, 1967) to

$$\log(A/\sqrt{P}) = -b/2 \log(P_{1/2} + P) + b/2 \log(P_{1/2}) + \log(K) = -b/2 \log(P_{1/2} + P) + \text{constant} \quad (4)$$

The value of $P_{1/2}$ can be determined from progressive saturation experiments (Oliver & Hales, 1992) by fitting eq 4 to plots of experimental data of $\log(A/\sqrt{P})$ vs $\log P$.

Distance Determination: Theory. Equation 2 demonstrates that the magnitude of the magnetic interaction experienced by species *i* is related to $1/T_{1i}$. Since relaxation rates are additive

$$(1/T_{1i})_{\text{measured}} = (1/T_{1i})_{\text{intrinsic}} + (1/T_{1i})_{\text{dipolar}} \quad (5)$$

where $(1/T_{1i})_{\text{intrinsic}}$ is the rate in the absence of perturbing species *j* while $(1/T_{1i})_{\text{dipolar}}$ is the rate in its presence. Using eq 3 and assuming a constant T_{2i}, eq 5 can be rearranged to

$$(P_{1/2})_{\text{dipolar}} = \Delta P_{1/2} = (P_{1/2})_{\text{measured}} - (P_{1/2})_{\text{intrinsic}} \quad (6)$$

Therefore, according to eq 2

$$\Delta P_{1/2} \propto (1/T_{1i})_{\text{dipolar}} \quad (7)$$

or

$$\Delta P_{1/2} \propto 1/r^6 \quad (8)$$

In eq 8, it is assumed that species *i* interacts with a single species *j* at a distance *r*. For more than one species *j* at a concentration [*j*]

$$\Delta P_{1/2} = K\sum_j r^{-6} = K'[j]\{r^{-6}\} \quad (9)$$

where *K* and *K'* are constants dependent on the spectroscopic properties of species *i* and *j* and $\{r^{-6}\}$ represents an effective distance for the ensemble of species *j*. The value of *K'* can be determined by using paramagnetic protein standards and has been found to be temperature-dependent. For example, when species *j* is DyEDTA, eq 9 can be rewritten (Blum et al., 1981) as

$$\Delta P_{1/2} = C \exp^{-12.5/T}[\text{DyEDTA}]\{r^{-6}\} \quad (10)$$

where constant *C* is now temperature-independent.

The difficulty in using eq 10 to evaluate experimental data has been in the interpretation of the meaning of $\{r^{-6}\}$. In early models (Blum et al., 1980, 1981, 1983; Blum & Ohnishi, 1980; Hyde & Rao, 1978), this effective distance was associated with either the distance from a protein-bound paramagnetic center to the nearest Dy^{3+} or the weighted average distance of the paramagnetic center to all the surface-bound Dy^{3+} ions (in both cases, the summation $\{r^{-6}\}$ was replaced by a single average distance $[r_{\text{ave}}]^{-6}$). Using this approach (called model 1) and assuming a distance $X = 5$ Å for the radius of DyEDTA, eq 10 has been simplified (Blum et al., 1981) to

$$\Delta P_{1/2} = (4.12 \times 10^8) \exp^{-12.5/T}[\text{DyEDTA}]r^{-6} \quad (11)$$

Recently, a more detailed approach has been used (Innes & Brudvig, 1989) to determine $\{r^{-6}\}$ by replacing $\sum_j r^{-6}$ in eq 9 with the integration of r^{-6} over the structure of a spheroidal protein assuming either surface binding (model 2) or a random distribution in solution (model 3) of DyEDTA. The problem

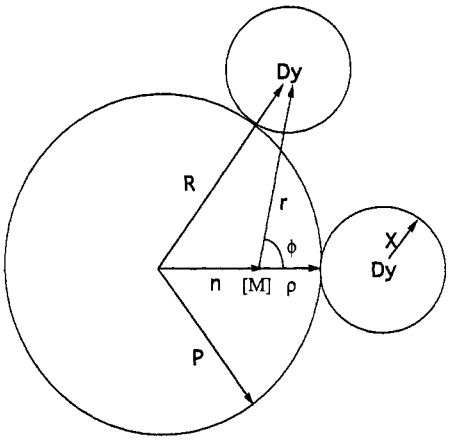

FIGURE 1: Spherical protein model used in the text for models 2 and 3. This model has a radius P and contains a paramagnetic cluster [M] a distance n from the center. Two perturbing DyEDTA complexes are shown, one at the point of closest contact, a distance ρ from [M], while the second complex has the dysprosium ion a distance r, from [M] and a distance R from the center of the protein.

associated with using this approach is that the structural dimensions of the spheroidal protein must be known, which is typically not the case.

A simplified version of models 2 and 3 will be used to circumvent this problem. Assuming the protein to be spherical (instead of spheroidal) with a radius P (Figure 1), the intrinsic paramagnet [M] is displaced a distance n from the center of the sphere (and, therefore, a distance $\rho = P - n$ from the nearest surface). The distance r of the protein-bound paramagnetic to any Dy^{3+} on the surface of the protein is dependent only on the angle ϕ between the vector along r and the vector along P through the paramagnet and can be expressed as

$$r = n\cos\phi + [n^2\cos^2\phi + (R^2 - n^2)]^{1/2} \qquad (12)$$

where R ($=P + X$) is the distance of closest approach of the Dy^{3+} ion to the center of the protein and X is the radius of the DyEDTA complex. The value of $\{r^{-6}\}$ can be determined by simple numerical integration of either

$$\{r^{-6}\}_{\text{model 2}} = 2\pi\int_0^{\pi}\sin\phi\, d\phi/\{n\cos\phi + [n^2\cos^2\phi + (R^2 - n^2)]^{1/2}\}^4 \qquad (13)$$

assuming only surface binding or

$$\{r^{-6}\}_{\text{model 3}} = 2\pi/3\int_0^{\pi}\sin\phi\, d\phi/\{n\cos\phi + [n^2\cos^2\phi + (R^2 - n^2)]^{1/2}\}^3 \qquad (14)$$

for a random distribution in solution. Using the values of these integrals along with the empirical dependency of $\Delta P_{1/2}$ on [DyEDTA] in eq 10 allows us to predict the value of n and, therefore, ρ. [In those situations where the value of P is unknown, it can be approximated (in Å) for a spherical protein of known molecular weight using $R = 0.663(\text{mol wt})^{1/3}$.]

RESULTS

Fe-Protein. Similar to many reduced ferredoxins, component 2 possesses a rhombic EPR spectrum with $g_{ave} < 2$. Microwave power- and temperature-dependent studies on this spectrum (Watt & McDonald, 1985) suggest it exhibits anomalous saturation, especially at temperatures below 8 K. Because of this, all data were recorded at 8 K or above.

In the presence of DyEDTA, the saturation profile of Av2 is augmented, implying the existence of dipolar interaction.

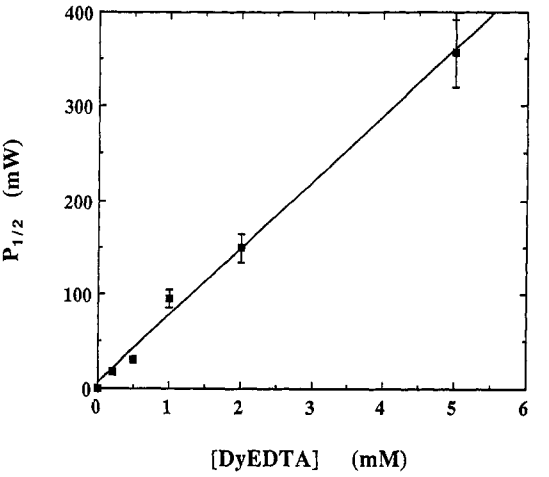

FIGURE 2: Dependency of the value of $P_{1/2}$ for the $g = 1.94$ line of Av2 on the concentration of DyEDTA in solution. Experimental conditions: temperature, 8 K; microwave frequency, 9.48 GHz; modulation amplitude, 10 G.

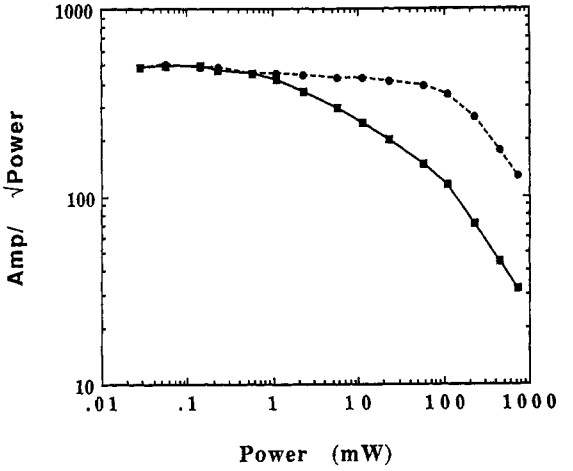

FIGURE 3: Example of a saturation profile (i.e., amplitude of the EPR intensity over the square root of the microwave power) of the $g = 2.25$ line of cytochrome c measured both by itself (solid line) and in the presence of 5 mM DyEDTA (dashed line). Experimental conditions: temperature, 4.4 K; microwave frequency, 9.46 GHz; modulation amplitude, 12.6 G.

Figure 2 shows the linear dependency of $P_{1/2}$ for Av2 on the concentration of DyEDTA. These data were not significantly affected by the presence of either NaCl (0.05–0.20 M) or the diamagnetic lanthanide complex LaEDTA. Furthermore, no DyEDTA-dependent spectral broadening of Av2 was observed in this concentration range. The slope of this graph is $\Delta P_{1/2}/[\text{DyEDTA}] = 71$ mW/mM. Using this value in eq 11 for model 1 yields $\rho_{\text{model 1}} = 5.0$ Å for the distance of the center of the [4Fe-4S] cluster to the point of closest approach of DyEDTA.

Before ρ can be calculated for models 2 and 3, the value of C in eq 10 must be determined through the use of a paramagnetic standard. In the past, horse heart cytochrome c, the high-potential iron–sulfur protein from *Chromatium vinosum*, and myoglobin nitroxide have been employed (Blum et al., 1980, 1981, 1983) as structural standards of soluble paramagnetic proteins. For example, Figure 3 shows the saturation profile of cytochrome c in the presence and absence of 5.0 mM DyEDTA. Using this standard along with its structural parameters $R = 17.5$ Å and $n = 8.5$ Å to determine the numerical integrations in eqs 13 and 14, the constants $C_{\text{model 2}} = 2.05 \times 10^6$ mW mM^{-1} Å^4 and $C_{\text{model 3}} = 5.38 \times 10^5$ mW mM^{-1} Å^3 can be obtained from eq 10. The effective

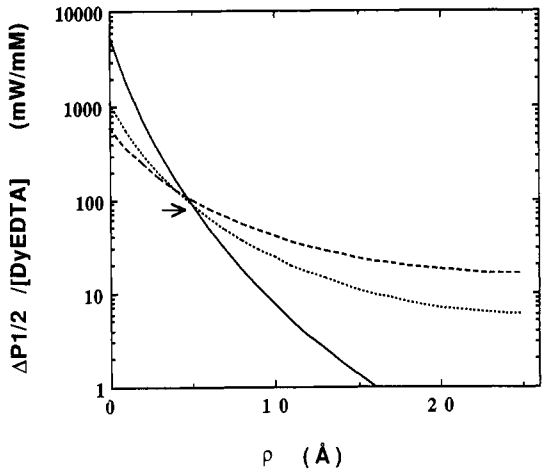

FIGURE 4: Theoretical prediction of the slope $\Delta P_{1/2}/[\text{DyEDTA}]$ determined for Av2 at 8 K as a function of ρ for model 1 (solid line), model 2 (dotted line), and model 3 (dashed line). These plots were determined by evaluating eq 13 in the text for model 1 or by numerical integration of eq 15 for model 2 or eq 16 for model 3. The arrow points to the experimental value of 71 mW/mM for the slope of Av2 at 8 K.

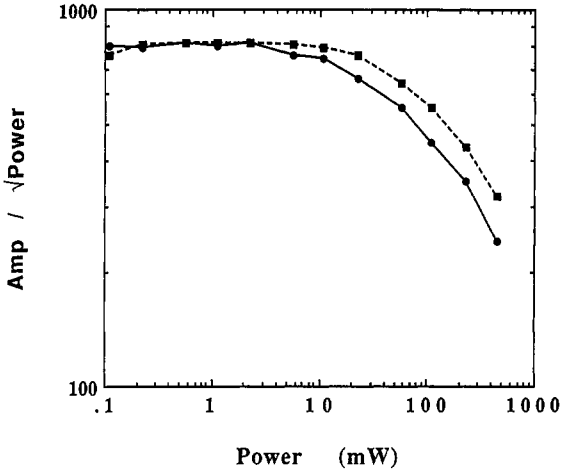

FIGURE 5: Example of a saturation profile for the $g = 3.65$ line of Av1 by itself (solid line) and in the presence of 1 mM DyEDTA (dashed line). Only part of all of the data is shown for clarity. Experimental conditions: temperature, 3.8 K; microwave frequency, 9.46 GHz; modulation amplitude, 12.6 G.

distances for Av2 then become $\{r^{-6}\}_{\text{model 2}} = 0.000165$ Å^{-4} and $\{r^{-6}\}_{\text{model 3}} = 0.000636$ Å^{-3}. Numerical integration of eq 13 and 14 using $R = 31$ Å for Av2 shows that $n_{\text{model 2}} = 19.5$ Å and $n_{\text{model 3}} = 20.3$ Å or, in other words, $\rho_{\text{model 2}} = 5.7$ Å and $\rho_{\text{model 3}} = 6.5$ Å for the distances assuming either surface binding or a random distribution in solution, respectively. Another way of visualizing these results is shown in Figure 4 where the theoretical variation of $\Delta P_{1/2}/[\text{DyEDTA}]$ is plotted as a function of ρ for the three different models. It can be seen from these plots that all three models place the [4Fe-4S] cluster very near the surface of Av2.

MoFe-Protein. In the as-isolated form, Av1 exhibits (Münck et al., 1975) a paramagnetism assigned to the ground state of an $S = {}^3/_2$ spin system having $D = +6.0$ cm^{-1} with spectral inflections at $g = 4.32$, 3.68, and 2.01. The origin of this paramagnetism is the M-center or FeMoco, believed to be at or near the site of substrate reduction. Because this cluster has $S > {}^1/_2$ with a low-energy excited state, spin relaxation is much more efficient than that observed for the $S = {}^1/_2$ signal of Av2, and pumped liquid He temperatures were required before significant spectral saturation was observed. Therefore, all spectra were recorded at 3.8 K. Various modulation frequencies were employed to assure the lack of saturation transfer effects.

Figure 5 shows an example of the effect of DyEDTA on the saturation profile of Av1. As was found for Av2, no dipolar-induced spectral broadening was observed, and there is a similar linear relationship between $P_{1/2}$ and [DyEDTA] with a slope of 280 mW/mM. The magnitude of this slope is by far the largest ever published. Using eq 11 with this value yields $\rho_{\text{model 1}} = 1.2$ Å for the distance of the center of FeMoco to the point of closest approach of DyEDTA, a result too small to be physically realistic. Similarly, in the second and third models, the effective distances for Av1 are calculated to be $\{r^{-6}\}_{\text{model 2}} = 0.0037$ Å^{-4} and $\{r^{-6}\}_{\text{model 3}} = 0.014$ Å^{-3}. Numerical integration of eq 13 and 14 using $R = 40$ Å yields $\rho_{\text{model 2}} = \rho_{\text{model 3}} = 0.0$ Å, results similar to that obtained with model 1. Interpretation of these unusually short distances will be presented under Discussion.

Cross-Linked Proteins. Having determined the saturation parameters for both Av1 and Av2 separately, the effect that different combinations of these two proteins (or with either Cp1 or Cp2) have on their respective parameters was also investigated. The first combination studied was the complex created by the chemical cross-linking of Av2 to Av1. The cross-linking of these two proteins (Av1–Av2) is an MgATP-independent process that binds one of the γ-polypeptides on Av2 with one of the β-polypeptides on Av1, producing an enzymatically inactive complex (Willing & Howard, 1990; Willing et al., 1989). Formation of Av1–Av2 was verified by SDS–PAGE which showed the presence of a band at $M_r = 97\,000$, indicative of the cross-linked β- and γ-polypeptides. In this study, duplicate Av1–Av2 samples were prepared, with and without DyEDTA, and the saturation profiles of both Av1 (at 3.8 K) and Av2 (at 8 K) recorded. Table I lists the effects of [DyEDTA] on $P_{1/2}$ for different preparations of Av1, demonstrating that, within experimental uncertainty, Av2 cross-linked to Av1 has no significant effect on the saturation behavior of FeMoco in the latter protein. Analogous results were obtained when the saturation properties of Av2 were monitored (Table I), signifying that cross-linking Av1 with Av2 does not measurably alter the interactions of the paramagnetic centers in either protein with DyEDTA.

Table I: Influence of DyEDTA on the Saturation Profile of the Nitrogenase Component Proteins

	$\Delta P_{1/2}/[\text{DyEDTA}]^a$	
sample	component 1	component 2
Av1	240	
Av2		74
Av1 + Av2[b]	230	80
Av1–Av2[c]	250	90
Av1–Cp2[d]	<20	<10
Cp1 + Av2[b]	240	85

[a] Units of mW/mM; error ≈ 20%. [b] Mixture of component 1 with component 2 in a 1:2 ratio. [c] Cross-linked Av1 with Av2 in a 1:2 ratio. [d] Enzymatically inactive, tight-binding complex formed between Av1 and Cp2 in a 1:2 ratio.

Heterologous Mixtures. It has long been known (Emerich & Burris, 1976, 1978; Emerich et al., 1978; Smith et al., 1976) that mixing one nitrogenase component protein from *A. vinelandii* with the complementing protein from *C. pasteurianum* yields enzymatically inactive systems. Studies of these heterologous matches have shown that mixing Av1 with Cp2 generates a tight-binding inactive complex while Cp1 combined with Av2 simply produces an enzymatically inactive mixture. To better understand these systems, the

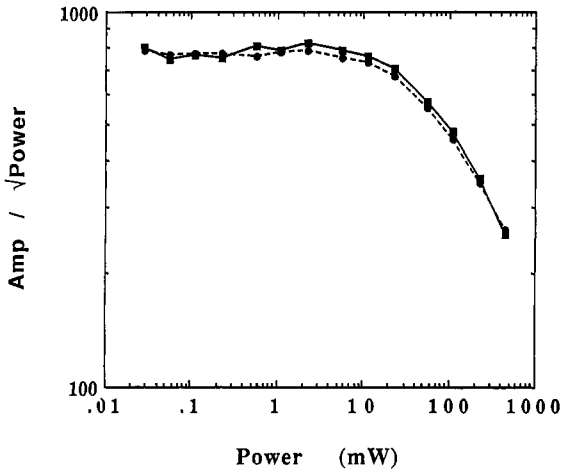

FIGURE 6: Saturation profile of the $g = 3.64$ line of Av1 in the complex Av1–Cp2 (1:2 molar ratio) by itself (solid line) and in the presence of 1.0 mM DyEDTA (dashed line). Only part of the saturation data is shown for clarity. Experimental conditions: temperature, 3.8 K; microwave frequency, 9.46 GHz; modulation amplitude, 12.6 G.

effect of added DyEDTA on the saturation profiles of the two component proteins in either of these heterologous systems was investigated.

Figure 6 shows that Cp2 effectively blocks the influence of DyEDTA on the saturation profile of Av1. The lack of a DyEDTA-induced increase in $P_{1/2}$[Av1] suggests that in the tight-binding complex (Av1–Cp2) Cp2 shields FeMoco, significantly increasing the distance between it and the nearest DyEDTA. An analogous effect is observed in the saturation profile of Cp2 in the complex (Table I). On the other hand, when the mixture of Av2 with Cp1 was investigated, no significant change was observed in $\Delta P_{1/2}$ for either protein (Table I). In other words, the extent of the dipolar interaction between DyEDTA and the metal clusters of either Av2 or Cp1 is unaffected by the presence of the other protein.

DISCUSSION

Lanthanide ions have been used in the past (Blum et al., 1980, 1981, 1983; Blum & Ohnishi, 1980; Hyde & Rao, 1978) to perturb intrinsic membrane- and protein-bound paramagnets. The result of this perturbation is often a spectral line broadening and/or increase in the spin–lattice relaxation rate (eq 2) of the intrinsic center. Assuming an interaction that is mainly dipolar in origin, expressions have been derived (Blum et al., 1981; Blum & Ohnishi, 1980; Hyde & Rao, 1978) relating the magnitude of the increase in relaxation rate with the spectroscopic parameters of both the perturbing and intrinsic paramagnets. For a single pair of paramagnets, this perturbation has a r^{-6} dependency. Under more typical conditions, where many perturbing ions interact with the same intrinsic center, the final expression (eq 9) for the total interaction is obtained by summing the interactions for each ion. This summation has been represented (Blum et al., 1981; Blum & Ohnishi, 1980; Hyde & Rao, 1978) either as a single distance or, more recently (Innes & Brudvig, 1989), as an integration of the distance over all the possible sites for the perturbing ion assuming either surface binding or a random distribution in solution. Unlike the single-distance model (r^{-6}), these latter models have distance dependencies of r^{-4} (eq 13) or r^{-3} (eq 14). Obviously, in these latter models, the extent of perturbation is less sensitive to the distance of the intrinsic paramagnet to the surface of the protein. A problem encountered with these latter models (Innes & Brudvig, 1989), but not present in the first, is the need to know the structural dimensions of the protein under study. We have circumvented this complication by assuming a simple spherical model for our proteins. With this assumption, only the radius of the protein need be known.

What are the ramifications of this assumption? Model 1 states that this assumption is unimportant since the perturbation is dependent only on a single effective distance of the intrinsic paramagnet to the surface and, therefore, is independent of the structure of the protein. To demonstrate the effect of this assumption on the second (surface-binding) and third (random distribution) models, a simple calculation can be performed. Assume a random distribution of DyEDTA in solution and an intrinsic paramagnet 5 Å from the surface ($\rho = 5$ Å) of a protein whose radius is 20 Å ($P = 20$ Å), being perturbed by DyEDTA with a radius of 5 Å (therefore, $X = 5$ Å and $R = 25$ Å). Using these parameters, eq 13 tells us that $\{r^{-6}\}_{\text{model 2}} = 0.0010$ Å^{-3}. If we now assume that the protein is actually 25 Å in radius, a back-calculation using this value of $\{r^{-6}\}_{\text{model 2}}$ yields a distance of $\rho = 4.5$ Å. In other words, a 5-Å increase in P resulted in a 0.5-Å decrease in the prediction of ρ. Therefore, the exact value of the protein's radius is not extremely critical in our determination of ρ. Similarly, it follows that the recent (Innes & Brudvig, 1989) use of 6.1 Å instead of 5.0 Å for the radius of the DyEDTA complex will have very little significant effect on the resultant calculation of ρ, so long as the same radius is used in the determination of the magnitude of C in eq 10 using standard proteins.

The determination of the exact value of the slope $\Delta P_{1/2}$/[DyEDTA] is also not very critical. For example, in model 1 an uncertainty of ±60% in the slope yields an uncertainty of only ±10% in the calculated value of ρ. We can, therefore, assume that the values of ρ predicted for Av1 and Av2 have an uppermost error of about ±20% for each of the three models used. Since it is presently unknown which of the three models best represents the correct physical situation, the distances calculated from all three will be taken as the range of acceptable values.

Fe-Protein. The range of values of ρ calculated from the three different models for Av2 is 5.0–6.5 Å. Since the paramagnetic center in Av2 is a [4Fe-4S] cluster with average distances (Stout, 1982) $r_{\text{Fe–Fe}} = 2.7$ Å, $r_{\text{S–S}} = 3.6$ Å, $r_{\text{Fe–S}} = 2.3$ Å, and $r_{\text{Fe–S(Cys)}} = 2.2$ Å, the approximate distance from the center of the cluster to a neighboring S(Cys) is about 4.0 Å. Therefore, the results presented here suggest that the edge of the [4Fe-4S] cluster of Av2 is 2–3 Å from the point of closest approach of DyEDTA, a result in agreement with the recent X-ray diffraction studies (Georgiadis et al., 1990, 1992) showing the cluster bridged between the two γ-polypeptides and very near the outside edge of the protein. Our calculated distance, being greater than a normal bond length, suggests an explanation for the inability of external chelators to react with the Fe in the cluster (Ljones & Burris, 1978). Since this chelation reaction occurs rapidly in the presence of MgATP, we can hypothesize that MgATP binding to Av2 induces a slight conformational change to shortening this distance to about 1–2 Å, thereby allowing chelation to occur. Unfortunately, attempts by us to test this hypothesis by recording Av2–MgATP saturation profiles with and without added DyEDTA proved inconsistent, possibly due to DyEDTA inhibition of the binding of MgATP.

MoFe-Protein. The range of values of ρ calculated from the three different models for Av1 is 0.0–1.2 Å. These predicted distances are obviously unrealistically small and

result from the unprecedented large value of the slope $\Delta P_{1/2}$/[DyEDTA] = 280 mW/mM. To understand the source of the discrepancy, we must look back at the original derivation of eq 10 from eq 2. It has been shown (Hyde & Rao, 1978) that when DyEDTA is used to perturb the relaxation rate of a free radical (i.e., $S = {}^1/_2$ species), the c term in eq 2 becomes the dominant term. This occurs because $1/T_1$ for DyEDTA is of the order of magnitude of ω for the free radical, or $\omega_i T_{1j} \approx 1$ in the denominator of the c term, making it the dominant term. Therefore, as long as the paramagnetic standard and unknown are both $S = {}^1/_2$ states, the constant C in eq 10 will be influenced mainly by the c term in eq 2, will be the same for both the standard and the unknown, and can be used in the calculation of ρ for the unknown.

This is not the case for the cofactor of Av1 where the paramagnetism arises for an $S = {}^3/_2$ state. There are three terms in eq 2 that depend on the spin state of the unknown (species i). These are γ_i, ω_i, and ϕ_{ij}. The magnetogyric ratio (γ_i) of an $S = {}^3/_2$ state is about twice that of an $S = {}^1/_2$ state, which will increase all of the terms in eq 2 by a factor of 4. The precession frequency of an $S = {}^3/_2$ state (ω_i) is similarly also greater than that of an $S = {}^1/_2$ state. As ω_i increases, it will start to approach that of DyEDTA (ω_j) such that the b term in eq 2 will gain greater significance and will eventually become the dominant term, overriding the c term. This effect is important because the b term has a larger angular contribution [$(1 - 3\cos^2\phi_{ij})^2$] than does the c term ($\sin^2\phi_{ij}\cos^2\phi_{ij}$). In fact, in the extreme case where the b term completely replaces the c term, the average angular contribution along with the larger magnetogyric ratio could increase the proportionality constant C in eq 10 by a factor of 76. For the sake of comparison, let us assume that C in eq 10 for the $S = {}^3/_2$ signal of Av1 has increased by a factor of 25, as a lower limit (a reasonable increase, in light of the above discussion). Using this value of C would generate new effective distances of $\{r^{-6}\}_{\text{model 2}} = 0.000148$ Å^{-6} and $\{r^{-6}\}_{\text{model 3}} = 0.00056$ Å^{-3}, yielding $\rho_{\text{model 1}} = 5.6$ Å, $\rho_{\text{model 2}} = 5.6$ Å, and $\rho_{\text{model 3}} = 6.4$ Å. Although the true increase of C is not known, these approximated distances suggest that FeMoco can be considered to be ≥6 Å to the surface in Av1. Recent X-ray diffraction studies (Kim & Rees, 1992a) on Av1 suggest that the correct distance is ~10 Å, implying an even greater contribution from the b term in eq 10 than the 33% used in our approximation.

Cross-Linked Proteins. Because the degree of perturbation of $P_{1/2}$ is related to the distance of closest approach of DyEDTA to the intrinsic paramagnetic center, forming complexes between the nitrogenase proteins may "hide" one or both of their paramagnetic clusters, increasing the distance of closest approach and decreasing the perturbation. A mixture of the normal catalytic pair (Av1 + Av2 in Table I) during nonturnover conditions showed no significant change in $\Delta P_{1/2}$/[DyEDTA] for either protein. One explanation of this result is that even though the association of Av1 and Av2 hides one or both of their clusters, too small a fraction of these proteins exists as associated complexes in the steady state to significantly affect $\Delta P_{1/2}$. Other possibilities are that the association of Av1 with Av2 does not hide either cluster or that the proteins only associate during enzymatic turnover. Unfortunately, the determination of the effect of DyEDTA on the saturation profiles of either of these proteins during enzymatic turnover could not be accomplished since DyEDTA inhibits nitrogenase activity.

One way of assuring the existence of a bound complex is through chemical cross-linking of Av1 with Av2. Previous results have shown (Willing et al., 1989) that EDC forms a linkage (Willing & Howard, 1990) between residues Glu-112 on Av2 and Lys-399 on the β subunit of Av1. Glu-112 is located in a loop that is directly C-terminal to the cluster helix of the [4Fe-4S] and is about 25 Å away from the cluster (Georgiadis et al., 1990, 1992). The lack of change in $\Delta P_{1/2}$/[DyEDTA] in the cross-linked enzyme (Table I) suggests that Av2 is tethered to Av1 but the [4Fe-4S] cluster is not masked. The same results hold for the $S = {}^3/_2$ signal of FeMoco in Av1. This latter result is not unexpected since Av2 is cross-linked to the β subunit of Av1 close to the P-clusters, while FeMoco is bound to the α subunit (Kim & Rees, 1992a).

Heterologous Mixtures. In the heterologous tightly-bound complex Av1–Cp2, we observe the first indication of cluster masking. The presence of bound Cp2 blocks the ability of DyEDTA (up to 1.0 mM) to induce any observable relaxation enhancement of FeMoco in Av1. Without DyEDTA, FeMoco in the complex has a $P_{1/2} = 190$ mW at 3.8 K. If we assume about a 10% error in the determination of this number, then the presence of DyEDTA may raise $P_{1/2}$ to 210 mW without our being able to detect any difference. We can, therefore, assume $\Delta P_{1/2}$/[DyEDTA] ≤ 20 mW as an upper limit for this change. Assuming again an approximate correction factor of 25 on C, we can assign a lower limit on the increase in the distance of FeMoco to the nearest DyEDTA of $\Delta\rho \geq 10$ Å. If Cp2 has the same dimensions as those published for Av2 (Georgiadis et al., 1990, 1992) (i.e., 40 Å × 45 Å × 75 Å), only a small portion of Cp2 need overlap FeMoco to produce the observed effect.

These latter results are significant because they suggest that the cross-linked complex Av1–Av2 and the heterologous complex Av1–Cp2 bind to different regions of the two proteins. It is important to note, however, that it is not known whether either of these complexes actually represents the interaction that occurs during normal catalytic turnover.

Finally, it was noted that the value of $P_{1/2}$ for Av1 (in the absence of DyEDTA) increased when the protein was complexed with Cp2. Specifically, Av1 alone has $P_{1/2} = 160$ mW at 3.8 K while in the complex Av1–Cp2 Av1 has $P_{1/2} = 190$ mW. This increase could be due either to the presence of dipolar interaction between FeMoco in Av1 and the [4Fe-4S] cluster in Cp2 or a slight structural change in Av1, induced from the complexing with Cp2, that changes the T_1 *and/or* T_2 of Av1 and, accordingly, $P_{1/2}$. We are unable to distinguish between these two possibilities.

REFERENCES

Abragam, A. (1955) *Phys. Rev. 98(6)*, 1729–1735.

Beinert, H., & Orme-Johnson, W. H. (1967) in *Magnetic Resonance in Biological Systems* (Ehrenberg, A., Malmström, B. G., & Vänngard, T., Eds.) pp 221–247, Pergamon Press, Oxford.

Bloembergen, N. (1949) *Physica 15*, 386–426.

Blum, H., & Ohnishi, T. (1980) *Biochim. Biophys. Acta 621*, 9–18.

Blum, H., Leigh, J. S., & Ohnishi, T. (1980) *Biochim. Biophys. Acta 626*, 31–40.

Blum, H., Cusanovich, M. A., Sweeney, W. V., & Ohnishi, T. (1981) *J. Biol. Chem. 256(5)*, 2199–2206.

Blum, H., Bowyer, J. R., Cusanovich, M. A., Waring, A. J., & Ohnishi, T. (1983) *Biochim. Biophys. Acta 748*, 418–428.

Bolin, J. T., Ronco, A. E., Mortenson, L. E., Morgan, T. V., Williamson, M., & Xuong, N.-H. (1990) in *Nitrogen Fixation: Achievements and Objectives* (Gresshoff, P. M., Roth, L. E., Stacey, G., & Newton, W. E., Eds.) pp 117–124, Chapman and Hall, New York.

Burgess, B. K., Jacobs, D. B., & Stiefel, E. I. (1980) *Biochim. Biophys. Acta 614*, 196–209.
Castner, T. G., Jr. (1959) *Phys. Rev. 115(6)*, 1506–1515.
Emerich, D. W., & Burris, R. H. (1976) *Proc. Natl. Acad. Sci. U.S.A. 73(12)*, 4369–4373.
Emerich, D. W., & Burris, R. H. (1978) *J. Bacteriol. 134(3)*, 936–943.
Emerich, D. W., Ljones, T., & Burris, R. H. (1978) *Biochim. Biophys. Acta 527*, 359–369.
Georgiadis, M. M., Chakrabarti, P., & Rees, D. C. (1990) in *Nitrogen Fixation: Achievements and Objectives* (Gresshoff, P. M., Roth, L. E., Stacey, G., & Newton, W. E., Eds.) pp 111–116, Chapman and Hall, New York.
Georgiadis, M. M., Komiya, H., Chakrabarti, P., Woo, D., Kornuc, J. J., & Rees, D. C. (1992) *Science 257*, 1653–1659.
Hales, B. J., Langosch, D. J., & Case, E. E. (1986) *J. Biol. Chem. 261(32)*, 15301–15306.
Hyde, J. S., & Rao, K. V. S. (1978) *J. Magn. Reson. 29*, 509–516.
Innes, J. B., & Brudvig, G. W. (1989) *Biochemistry 28*, 1116–1125.
Johnson, M. K., Thomson, A. J., Robinson, A. E., & Smith, B. E. (1981) *Biochim. Biophys. Acta 671*, 61–70.
Kim, J., & Rees, D. C. (1992a) *Nature 360(10)*, 553–560.
Kim, J., & Rees, D. C. (1992b) *Science 257*, 1677–1682.
Ljones, T., & Burris, R. H. (1978) *Biochemistry 17(10)*, 1866–1872.
Münck, E., Rhodes, H., Orme-Johnson, W. H., Davis, L. C., Brill, W. J., & Shah, V. K. (1975) *Biochim. Biophys. Acta 400*, 32–53.
Oliver, M. E., & Hales, B. J. (1992) *J. Am. Chem. Soc. 114*, 10618–10623.
Portis, A. M. (1953) *Phys. Rev. 91(5)*, 1071–1079.
Smith, B. E., Thorneley, R. N. F., Eady, R. R., & Mortenson, L. E. (1976) *Biochem. J. 157*, 439–447.
Stout, C. D. (1982) in *Iron–Sulfur Proteins* (Spiro, T. G., Ed.) pp 97–146, John Wiley & Sons, New York.
Watt, G. D., & McDonald, J. W. (1985) *Biochemistry 24*, 7226–7231.
Willing, A., & Howard, J. B. (1990) *J. Biol. Chem. 265*, 6596.
Willing, A. H., Georgiadis, M. M., Rees, D. C., & Howard, J. B. (1989) *J. Biol. Chem. 264*, 8499–8503.
Zimmermann, R., Münck, E., Brill, W. J., Shah, V. K., Henzl, M. T., Rawlings, J., & Orme-Johnson, W. H. (1978) *Biochim. Biophys. Acta 536*, 185–207.